Resonant magnetic x-ray scattering in UPd_2Si_2 at the uranium $L_{2,3}$ edges

D. Wermeille and C. Vettier
European Synchrotron Radiation Facility, Boîte Postale 220, 38043 Grenoble Cedex, France

N. Bernhoeft
European Synchrotron Radiation Facility, Boîte Postale 220, 38043 Grenoble Cedex, France
and Institut Max von Laue-Paul Langevin, Boîte Postale 156, 38042 Grenoble Cedex, France

A. Stunault*
European Synchrotron Radiation Facility, Boîte Postale 220, 38043 Grenoble Cedex, France

S. Langridge†
European Synchrotron Radiation Facility, Boîte Postale 220, 38043 Grenoble Cedex, France
and European Commission, Joint Research Center, Institute for Transuranium Elements, Postfach 2340, D-76125 Karlsruhe, Federal Republic of Germany

F. de Bergevin
Laboratoire de Cristallographie, CNRS, Boîte Postale 166, 38042 Grenoble Cedex, France

F. Yakhou
European Synchrotron Radiation Facility, Boîte Postale 220, 38043 Grenoble Cedex, France

E. Lidström
European Synchrotron Radiation Facility, Boîte Postale 220, 38043 Grenoble Cedex, France
and European Commission, Joint Research Center, Institute for Transuranium Elements, Postfach 2340, D-76125 Karlsruhe, Federal Republic of Germany

J. Flouquet
Commissariat à l'énergie atomique, DRFMC, SPSMS, 38054 Grenoble Cedex, France

P. Lejay
Centre de Recherche sur les Très Basses Températures, CNRS, Boîte Postale 166, 38042 Grenoble Cedex, France
(Received 3 April 1998)

The nature of the resonant magnetic x-ray-scattering processes at the uranium L_2 and L_3 edges of UPd_2Si_2 has been studied. The different polarization dependences of the electric dipole and quadrupole transitions are used to distinguish the two channels. The temperature variation, together with the angular dependence of the magnetic reflections demonstrate the dipolar origin of the resonance at the uranium L_2 and L_3 edges of UPd_2Si_2. Resonant magnetic x-ray scattering at these edges thus explores the spin polarization of the valence $6d$ band and allows the study of the magnetism of electronic d orbitals separately from f levels probed at the M_4 and M_5 edges in dipole transitions. The energy profiles of the two L edges are different. A single resonance is observed at the L_2 edge. The line shape at the L_3 edge shows two distinct contributions, both of dipolar type, which may be due to the influence of the core hole on the density of states of $6d$ levels. The energy of the maximum of the resonant intensity in both profiles corresponds to the inflexion point in the respective absorption coefficient curve. An effort to put the scattering amplitudes on an absolute scale has been made in order to compare with theoretical calculations. [S0163-1829(98)07037-4]

I. INTRODUCTION

Intermetallic uranium compounds UT_2Si_2, where T is a transition metal, form a class of materials with remarkable magnetic and electronic properties ranging from heavy-fermion and superconducting states to ferro- and antiferromagnetism or even Pauli paramagnetism. In these compounds, the hybridization of the $5f$ uranium states with the T d states and the relative position of these two narrow and tight-binding bands are critical:[1] they determine the existence of spontaneous magnetization at the uranium and T sites. In that respect, the role of the uranium $6d$ states appears less important, the $6d$ bands being much broader and having lower density of states at the Fermi level. However, the uranium d electrons exhibit a weak magnetic polarization,[2] which is difficult to detect directly by neutron diffraction or magnetization measurement. Resonant magnetic x-ray scattering (RMXS), which is species and electronic shell sensitive may be a more appropriate tool. This method offers a probe to investigate induced magnetic moments (on the T sites for example) and to compare f and d polarization on a given site. Indeed, RMXS has become a common and pow-

erful method to investigate electronic and magnetic properties in solids.[3–5] This technique takes advantage of the enhancement of the elastic magnetic scattering cross section when the incident photon energy is tuned through an appropriate absorption edge of the element under study. The magnetic scattering arises from electric multipole transitions from core levels to unoccupied spin-polarized electronic states. The amplitude is related to the spin-polarization and spin-orbit splitting of the initial and intermediate states and the multipole overlap integral (hereafter simply called the overlap integral) of the intermediate levels with the initial and final electronic orbitals. The effect is large at the uranium M_4 and M_5 edges because dipole transitions from the $3d_{3/2}$ and $3d_{5/2}$ core levels probe the large spin polarization of the partially filled $5f$ states. Furthermore, there exists large overlap integrals between $3d$ and $5f$ orbitals, the resonant amplitude reaching 9 r_0 at the uranium M_4 edge in UAs,[6] where $r_0 \approx 2.82 \times 10^{-5}$ Å is the classical radius of the electron. At the uranium L edges, where the initial states are the $2p_{1/2}$ and $2p_{3/2}$ for the L_2 and L_3 edges, respectively, the scattering amplitude is weaker. At these edges, dipole transitions connect the $2p$ core levels to the valence $6d$ band. The magnetic sensitivity arises from the spin-orbit splitting of the initial state. Rough estimates give a scattering amplitude of a few 10^{-2} r_0.[7,8] Quadrupole transitions would probe more strongly the polarized $5f$ states but have weaker overlap integrals, which reduces the scattering amplitude to the same few 10^{-2} r_0.[8]

Since the predicted scattering amplitudes for both dipole and quadrupole transitions have similar magnitudes, only experimental investigations of the resonance can establish the nature of the transitions. The purpose of this work is to observe the contributions from the $6d$ electronic orbitals of uranium to RMXS. This can be achieved by demonstrating the dipolar character of the transitions at the $L_{2,3}$ edges.

The weak enhancement expected at the uranium L edges and experimental difficulties account for the absence of work reported in the literature. Most of experiments on the d shell polarization and theoretical developments have been pursued at the L edges of rare-earth compounds, where both x-ray magnetic circular dichroism[9] and resonant exchange scattering[10] experiments give promising results for the understanding of the role of the $5d$ electrons in the magnetic properties of these compounds.

UPd_2Si_2 crystallizes in the body-centered-tetragonal $ThCr_2Si_2$ structure with space group $I4/mmm$. It undergoes successive magnetic phase transitions as a function of temperature.[11] In a preliminary x-ray-scattering experiment[12] on the sample used in this work, we have evidenced the following features while cooling. Below $T_N = 136$ K, an incommensurate magnetic phase appears, whose wave vector $\mathbf{q} = [0\ 0\ q_z(T)]$ is temperature dependent and parallel to the c^* axis of the tetragonal structure. At all temperatures, the magnetic ordered moments lie along the c axis. In the interval $125\ \mathrm{K} > T > 105$ K, this magnetic structure coexists with a second incommensurate phase with a wave vector $q_z = 0.711$ r.l.u. and between 108 and 95 K, with a simple commensurate type-I antiferromagnetic phase. Below 95 K, the incommensurate phase, with a temperature-dependent wave vector, changes into a commensurate $q_z = 2/3$ r.l.u. phase. Finally, below 85 K there remains only the type-I antiferromagnetic structure, with alternate ferromagnetically ordered uranium sheets in the sequence $+-+-$ along the c axis. Neutron-diffraction experiments on single crystals[11] reported a saturated magnetic moment of $\mu = 2.3\mu_B$ per uranium atom in the low-temperature phase. Local spin-density-functional calculations[1] give a spin moment $\mu_s \approx 2\mu_B$ and an opposite orbital moment $\mu_l \approx -4\mu_B$ which makes a net magnetic moment around $\mu = 2\mu_B$ per uranium atom, close to the experimental value. Exchange interaction with the $5f$ states splits the $6d$ levels into spin-up and spin-down bands. This splitting results in a small induced $6d$ moment of about $0.2\mu_B$ per uranium atom.[2,13]

The paper is organized as follows. In Sec. II we describe the method and the experimental conditions. Results at the uranium L_3 and L_2 edges are presented in Sec. III. Then we develop the analysis of the energy line shape and the behavior as a function of scattering vector, polarization, and temperature of the resonant magnetic peaks. Finally we conclude that the magnetism of the $6d$ electrons in UPd_2Si_2 can be studied with x rays.

II. EXPERIMENTAL CONDITIONS

The high-purity single crystal used for this study was prepared by the Czochralski technique[14,15] and annealed for periods up to two weeks in ultrahigh vacuum (UHV). The sample was cut along a [0 0 1] face and annealed under UHV for one week at 950 °C. To improve the surface quality and to remove oxidized layers, the sample was polished and annealed again for one week in UHV at 950 °C. Sample characterization indicates a high crystalline quality. The mosaic spread is 0.040(2)° at 17 keV and the lattice parameters of the body-centered-tetragonal structure are $a = b = 4.083$ Å and $c = 10.048$ Å at $T = 20$ K.

The experiments were performed at the magnetic scattering beamline ID20 of the European Synchrotron Radiation Facility (ESRF, Grenoble, France).[16] The x-rays are provided by a 48 mm period linear, hybrid, undulator. The energy is selected using a double Si (111) crystal monochromator with sagittal focusing. The higher-order harmonic contamination of the beam is reduced by the use of two 1 m long rhodium coated mirrors with variable longitudinal focusing. The sample was mounted with the a^* and c^* axes in the vertical scattering plane in a ^{4}He closed-cycle refrigerator which allows measurements down to 12 K. The scattering geometry is illustrated in Fig. 1. At 17 keV, using the seventh harmonic of the undulator, the incident flux at the sample position is $\approx 1.5 \times 10^{12}$ photons/s at 100 mA with a beam size of 0.35×0.25 mm^2. The x rays were measured to be linearly polarized at $99 \pm 1\%$ in the plane of the storage ring, here referred to as the σ polarization plane. At 20 keV with the eighth harmonic of the undulator, the flux is $\approx 1 \times 10^{12}$ photons/s at 100 mA with a beam size of 0.5×0.5 mm^2. The degree of linear polarization was $98 \pm 1\%$. Contamination by the orthogonal π polarization was neglected at the two edges. The incident and diffracted beams were monitored by NaI(T1) scintillators.

The difficulty of experiments involving weak signals above a large background has led us to perform a polarization analysis of the scattered beam. Magnetic x-ray scattering processes, both resonant and nonresonant may rotate the in-

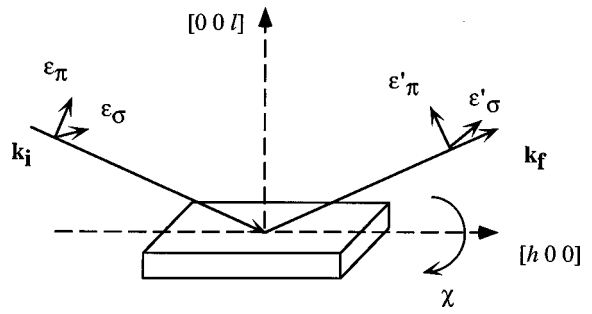

FIG. 1. Scattering geometry and directions in the reciprocal space. $\mathbf{k}_i$ and $\mathbf{k}_f$ are the incident and scattered wave vectors; $\boldsymbol{\epsilon}$ and $\boldsymbol{\epsilon}'$ denote the polarization vectors of the incident and scattered beams.

cident photon polarization, whereas the Thomson charge scattering does not change the polarization state of the incident beam. To perform polarization analysis,[17] a polarimeter was mounted on the detector arm. The device consists of a detector and suitable analyzer crystal with Bragg angle θ_a close to 45° at the nominal energy. With the analyzer diffraction plane coincident with that of the sample, the σ-polarized scattered x rays are measured. The analyzer crystal and the detector may be rotated together by 90° about the diffracted beam to detect the π-polarized scattered intensity. In addition to the separation of the two scattered polarization states, the analyzer crystal filters out fluorescence photons which have energy several hundreds of eV below the absorption edge. A LiF crystal makes a suitable analyzer for both the uranium L_2 and L_3 edges. The (0 0 8) LiF reflection gives an angle $\theta_a = 45.87(1)°$ at $E = 17.17$ keV with a reflectivity of about 1%. The (0 0 10) reflection corresponds to an angle $\theta_a = 47.34(1)°$ at $E = 20.945$ keV.

The origin of the observed background is twofold. First, there is an energy-dependent contribution coming from the fluorescence of the uranium atoms. Since the energy of the photons emitted in the fluorescence process is about 750 eV below the edge, this contribution to the background is considerably reduced by the energy bandpass of the analyzer crystal. The second contribution to the background comes from a ridge of elastic scattering along the c^* direction. This effect is illustrated in Fig. 2 where the normalized intensity of a scan along the h direction at the position of the magnetic (0 2 15) reflection is plotted as measured in the $\sigma \rightarrow \sigma$ channel at $T = 140$ K in the paramagnetic phase. The solid line is a Lorentzian square function with a full width at half maximum of about 0.002 r.l.u. centered at the Bragg position. k scans also show a similar peak. However, the scattered intensity collected in an orthogonal scan along the l direction is constant over a similar range (inset of Fig. 2). This is characteristic of ridges of charge scattering. The same measurements performed in the rotated $\sigma \rightarrow \pi$ channel did not reveal any measurable contribution along either h and l directions. Similar ridges have been observed in $\sigma \rightarrow \sigma$ for all specular (0 0 l) and off-specular (0 k l) or (h 0 l) magnetic reflections studied in this experiment. They may be related to reflectivity problems or coherent scattering effects due to the partial coherence of the synchrotron x-ray beam.[18]

In view of these effects and to take proper account of the magnetic contribution to the scattered signal, the magnetic integrated intensities discussed below have been extracted

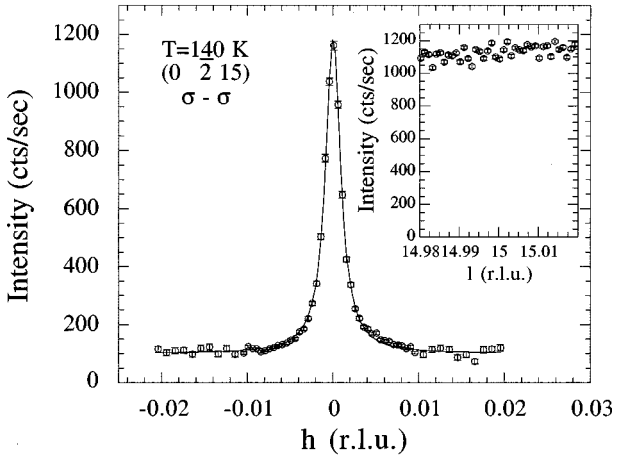

FIG. 2. h scan across the magnetic (0 $\bar{2}$ 15) reflection at $T = 140$ K in the paramagnetic phase measured in the unrotated $\sigma \rightarrow \sigma$ polarization channel. The solid line is a Lorentzian fit with a full width at half maximum of about 0.002 r.l.u. The inset shows the orthogonal l scan.

from l scans. Special care was taken to go far enough from the reflection for a correct determination of the background. The tabulated value for the uranium L_3 edge was used to calibrate the photon energy.

III. EXPERIMENTAL RESULTS

Figure 3 shows l scans across the magnetic (0 0 13) reflection in the $\sigma \rightarrow \pi$ channel for the paramagnetic ($T = 120$ K, closed circles) and the type-I antiferromagnetic ($T = 80$ K, open circles) phases performed at the uranium L_3 resonance, $E = 17.165$ keV. The magnetic signal represents about 30 counts/s at $T = 80$ K over a background of 0.3 count/s. Integrated intensity has been transformed into integrated reflectivity[19] I/I_0 by applying suitable corrections to the l scans.[20] In the case of an ideally imperfect extended crystal probed by a linearly polarized x-ray beam perpendicular to the scattering plane, the integrated reflectivity is given by[19]

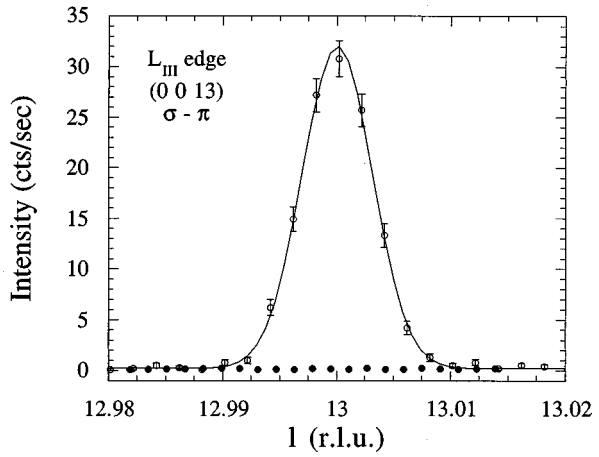

FIG. 3. l scan across the magnetic (0 0 13) reciprocal Bragg point at $T = 80$ K (○) and $T = 120$ K (●) in the $\sigma \rightarrow \pi$ channel at $E = 17.153$ keV, near the uranium L_3 resonance energy.

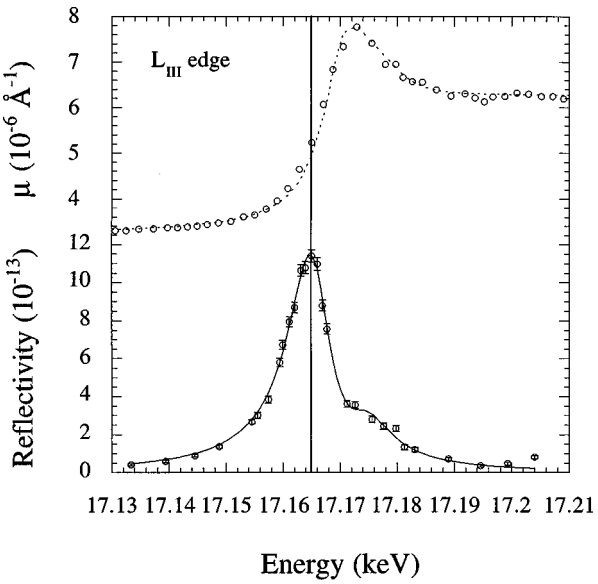

FIG. 4. Integrated reflectivity along the *l* direction of the magnetic (0 0 13) reflection at $T=80$ K in the rotated $\sigma\rightarrow\pi$ channel as a function of the incident photon energy around the L_3 edge. The solid line is a sum of two resonances centered at different energies. The upper part shows the absorption coefficient μ as determined from fluorescence. The dashed line corresponds to the analysis described in the text.

$$\frac{I}{I_0}=\frac{\lambda^3 r_0^2}{\mu^*\sin(\alpha)v_a^2}\frac{|F|^2}{\sin(2\theta)}, \tag{1}$$

where λ is the photon wavelength, F is the structure factor, $\mu^*=\mu[1/\sin(\alpha)+1/\sin(\beta)]$ with μ the absorption coefficient, α and β are the angles of the incident and scattered beams with the sample surface, and v_a is the unit-cell volume. The determination of the absorption coefficient μ near an absorption edge is a delicate problem when direct transmission measurement through a powder or a thin film of the studied material cannot be performed. It is possible, using simple assumptions about the fluorescence process to convert a fluorescence scan into the related absorption coefficient as a function of photon energy.[21–23] This determination is appropriate since the absorption corrections are not large at high incident photon energy (the penetration depth in UPd_2Si_2 is about 30 μm at the uranium $L_{2,3}$ edges). The observed intensities were corrected for the analyzer efficiency. The same data treatment was applied to all measured reflections.

A. Uranium L_3 edge

The reflectivity, integrated over *l*, of the magnetic (0 0 13) Bragg peak in the rotated $\sigma\rightarrow\pi$ channel is plotted in Fig. 4 as a function of the incoming photon energy around the L_3 edge. In the upper part, we show the absorption coefficient as deduced from fluorescence. The energy profile shows a strong resonance centered at $E=17.166$ keV, corresponding to the inflexion point in the absorption curve, followed by a weaker contribution, several eV above, at the maximum of the absorption coefficient. A similar energy dependence has been observed at the magnetic (1 0 14) reflection.

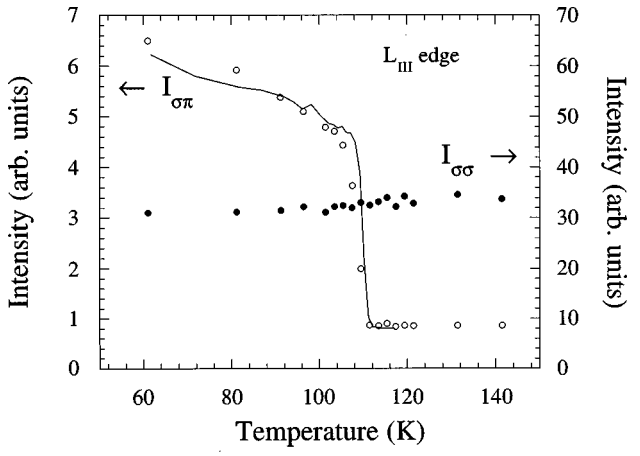

FIG. 5. Temperature dependence of the (0 $\bar{2}$ 15) in $\sigma\rightarrow\sigma$ (●) and $\sigma\rightarrow\pi$ (○) at $E=17.168$ keV, the resonance energy. The solid line is the temperature variation of the $5f$ ordered moment as deduced from RMXS at the uranium M_4 edge (Ref. 12).

At resonance, the integrated reflectivity is $(11.4\pm1)\times10^{-13}$, which can be translated into a scattering amplitude of $(3\pm0.5)\times10^{-2}$ r_0 per chemical unit cell. No magnetic scattering was observed when the photon energy differed from the resonant energy by more than 100 eV.

The temperature variation of the scattered signal in both unrotated $\sigma\rightarrow\sigma$ and rotated $\sigma\rightarrow\pi$ polarization channels was investigated at resonance for several magnetic Bragg peaks. The integrated scattered signal (including background) is shown in Fig. 5 for the (0 2 15) reciprocal-lattice point for both channels. In the $\sigma\rightarrow\pi$ channel, the scattered intensity vanishes at $T\approx108$ K, which corresponds to the Néel temperature of the (0 0 1) commensurate phase. Indeed, the $\sigma\rightarrow\pi$ amplitude follows the temperature variation of the $5f$ ordered moment (solid line in Fig. 5) as deduced from RMXS at the uranium M_4 edge.[12] In the $\sigma\rightarrow\sigma$ channel, the observed intensity is due to the ridge; there is no trace of any magnetic contribution since no change in intensity is observed at $T=108$ K.

Five off-specular reflections [(0 $\bar{1}$ 12), (0 $\bar{2}$ 13), (0 $\bar{2}$ 15), (0 3 16), and (0 4 17)] have been measured at $T=80$ K in the antiferromagnetic ordered phase and 150 K in the paramagnetic state, for both polarizations. We have performed these measurements at two different energies, one corresponding to the maximum of the resonant process ($E=17.166$ keV), the other being the maximum of the absorption curve, where the second contribution to the resonance profile is observed. At $T=80$ K, a magnetic signal has been detected for the five reflections in the $\sigma\rightarrow\pi$ channel, but nothing measured above background in the $\sigma\rightarrow\sigma$ channel for any reflection at both energies.

We have also measured several specular (0 0 *l*) Bragg peaks (with $l=5$, 7, 9, 11, 13) in the $\sigma\rightarrow\pi$ channel at the same energies. The corresponding magnetic integrated reflectivities are shown as a function of the corresponding Bragg angle, in Fig. 6(a) for $E=17.165$ keV and in Fig. 6(b) for $E=17.177$ keV. The monotonic increase in the magnetic structure factor, which is clearly observed will be discussed below.

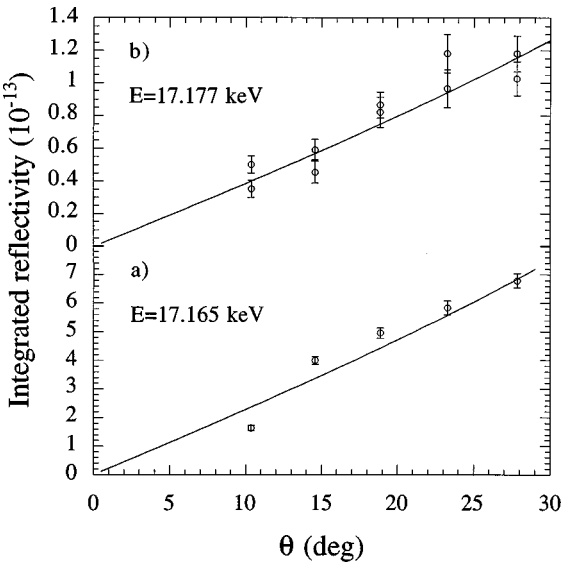

FIG. 6. Integrated reflectivity of the magnetic specular reflections (0 0 l) with $l=5$, 7, 9, 11, 13 as a function of the Bragg angle at $E=17.165$ keV at the maximum of the resonant signal (a) and at $E=17.177$ keV at the maximum of the absorption curve (b). The solid lines show the expected angular dependence of the scattering amplitude for dipole transitions.

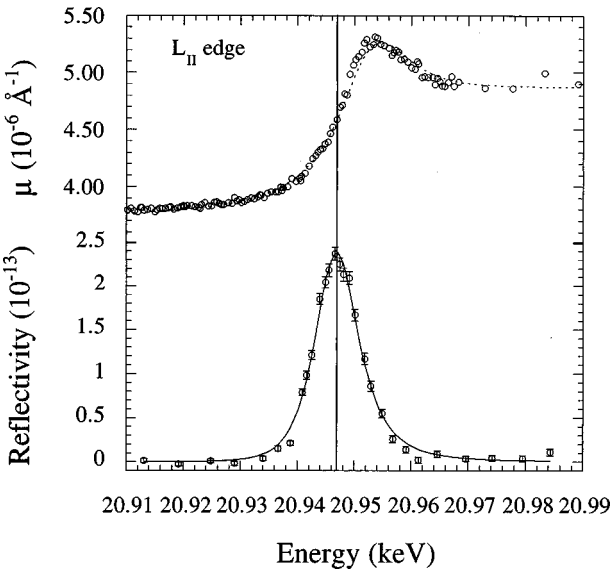

FIG. 8. Integrated intensity along the l direction of the magnetic (0 0 13) reflection at $T=80$ K in the $\sigma\rightarrow\pi$ channel as a function of the incident photon energy around the L_2 edge. The solid line corresponds to a splitting of 1 eV (see text). In the upper part the absorption coefficient μ is plotted as determined from fluorescence. The dashed line is obtained along the same assumptions as for the L_3 edge.

B. Uranium L_2 edge

Similar measurements were performed at the uranium L_2 edge. Ridges in $\sigma\rightarrow\sigma$ along the [0 0 l] direction were also observed. l scans across the (0 0 13) reflection in the $\sigma\rightarrow\pi$ channel at $E=20.945$ keV, near the uranium L_2 edge are shown in Fig. 7 in the antiferromagnetic phase ($T=80$ K) and the incommensurate phase ($T=120$ K). The magnetic signal was weaker compared with the L_3 edge and amounted to 7 counts/s. The energy-dependent integrated reflectivity is shown in Fig. 8 as measured in the $\sigma\rightarrow\pi$ polarization channel; the absorption coefficient as deduced from fluorescence is represented in the upper part of the figure. The resonance profile is different from the one observed at the L_3 edge. There is a single, well-defined contribution, centered at the inflexion point of the absorption curve. The integrated reflectivity at 20.946 keV corresponds to a scattering amplitude of $(1.5\pm0.5)\times10^{-2}\ r_0$. No magnetic scattering was detected when the incident energy was tuned more than 100 eV away from the L_2 edge.

The integrated intensity of the (0 0 13) and (0 $\bar{2}$ 15) magnetic peaks were measured for several temperatures around the (0 0 1) Néel point. A dependence similar to the one observed at the L_3 edge was evidenced. Again no magnetic contribution was detected at $T=80$ K in the $\sigma\rightarrow\sigma$ channel for either reflection. The specular (0 0 l) reflections (with $l=5$, 7, 9, 11, 13) were also measured at the resonance energy. Figure 9 shows their magnetic integrated reflectivities as a function of Bragg angle.

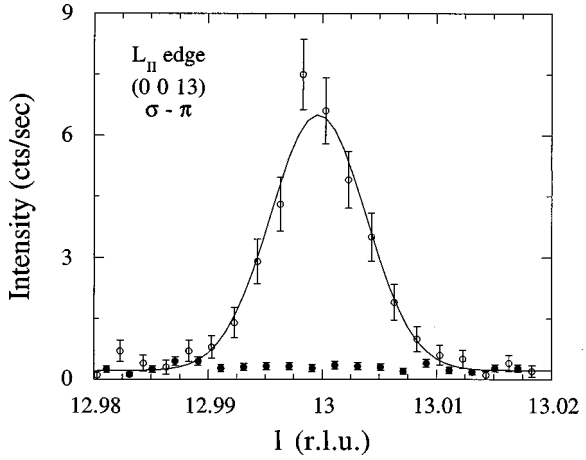

FIG. 7. l scan across the magnetic (0 0 13) reciprocal space position at $T=80$ K (○) and $T=120$ K (●) in the $\sigma\rightarrow\pi$ channel at $E=20.945$ keV, near the uranium L_2 resonance energy.

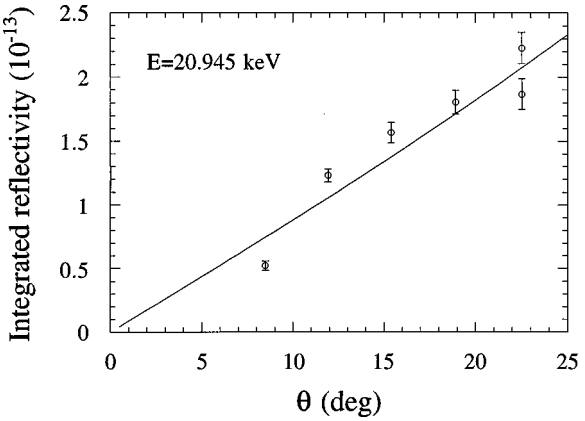

FIG. 9. Integrated reflectivity of the magnetic specular reflections (0 0 l) with $l=5$, 7, 9, 11, 13 as a function of the Bragg angle at the uranium L_2 edge. The solid line shows the expected angular dependence of the scattering amplitude for dipole transitions.

IV. DISCUSSION

We analyze the energy and the Q line shapes, and the polarization dependence of the scattered intensities in order to determine the nature (dipole versus quadrupole) of the resonance. The total magnetic x-ray scattering cross section contains a nonresonant part[24] and a resonant contribution.[7,25] As a test for internal consistency, we discuss the nonresonant scattering observed at 7.8 keV. The integrated reflectivity of the (0 0 9) magnetic Bragg reflection was 4×10^{-15}, which represents a scattering amplitude of $1.3\times10^{-3}\ r_0$.[12] The nonresonant magnetic scattering amplitude was calculated using expression derived by Blume and Gibbs.[26] With the reported spin moment of $2\mu_B$ per uranium atom in UPd_2Si_2 (Ref. 1) and the tabulated form factor for uranium,[27] the calculated scattering amplitude amounts to $1.34\times10^{-3}\ r_0$, in good agreement with the observation. The nonresonant scattering amplitudes for the (0 0 13) at $E=17$ and 21 keV are calculated in a similar manner and reach 4.8×10^{-4} and $3.2\times10^{-4}\ r_0$, respectively. These amplitudes are much lower than the resonant amplitudes observed at the L_2 and L_3 edges. First, this result explains why we do not observe any nonresonant signal near the $L_{2,3}$ edges. Second, it allows us to neglect the nonresonant amplitude in our analysis of the energy line shape.

A. Resonant line shape

Neglecting the nonresonant magnetic scattering amplitude, the structure factor F in Eq. (1) contains the usual Thomson and the resonant amplitude. For the resonant scattering two main processes should be considered: electric dipole and quadrupole transitions. First, let us consider electric dipole contributions that have been treated by Hannon *et al.*[7] in the case of atomic d states with no orbital moment. The magnetic contribution at the L_3 edge can be approximated by

$$f_{j,E1}^{L_3}=\frac{F_0^{L_3}}{x_{L_3}-i}\,[i(\boldsymbol{\epsilon}'\times\boldsymbol{\epsilon})\cdot\mathbf{z}_j P/4], \tag{2}$$

where $x_{L_3}=(E_{L_3}-\hbar\omega)/(\Gamma/2)$. The amplitude is given by

$$F_0^{L_3}=\frac{8}{45}\,\frac{mc^2}{\Gamma_{L_3}}\,(ka_0)^2|\langle 2p_{3/2}|r/a_0|6d\rangle|^2 r_0, \tag{3}$$

where a_0 is the Bohr radius and $\langle 2p_{3/2}|r/a_0|6d\rangle$ is an average matrix element for the $6d$ spin-up and spin-down orbitals. Γ is the total width for the excited state, as determined from the fluorescence curve. The magnetic moment of the jth atom is parallel to $\mathbf{z}_j$. $\boldsymbol{\epsilon}$ and $\boldsymbol{\epsilon}'$ are the incident and scattered photon polarization vectors. The polarization factor P is given by the asymmetry between spin-up and spin-down orbitals of the $6d$ bands. It contains the net $6d$ magnetic polarization, $n_{d\uparrow}-n_{d\downarrow}$, the asymmetry δ in the radial matrix elements for the $6d$ spin-up and spin-down states, and an exchange splitting, Δ. We have neglected any orbital moment in the $6d$ shell in presence of the core hole. In the limit where Δ/Γ is small, P can be written as:[8]

$$P=(n_{d\uparrow}-n_{d\downarrow})-n_h\delta-\frac{n_h\Delta/\Gamma}{(E_{L_3}-\hbar\omega)/(\Gamma/2)-i}, \tag{4}$$

where n_h is the number of holes of both spins in the $6d$ band. Some other terms could be considered, such as modifications of the density of states of the d levels in the presence of the core hole.

At the L_2 edge, the resonant amplitude has a similar form:

$$f_{j,E1}^{L_2}=\frac{F_0^{L_2}}{x_{L_2}-i}\,[-i(\boldsymbol{\epsilon}'\times\boldsymbol{\epsilon})\cdot\mathbf{z}_j P/2], \tag{5}$$

with

$$F_0^{L_2}=\frac{4}{45}\,\frac{mc^2}{\Gamma_{L_2}}\,(ka_0)^2|\langle 2p_{1/2}|r/a_0|6d\rangle|^2 r_0. \tag{6}$$

In this model, the ratio R of the magnetic resonant amplitude at the L_3 and L_2 edges is given by the widths Γ_{L_3}, Γ_{L_2}, the energy of the two edges and the radial matrix elements through the relation:

$$R=-\frac{|\langle 2p_{3/2}|r/a_0|6d\rangle|^2}{|\langle 2p_{1/2}|r/a_0|6d\rangle|^2}\,\frac{\Gamma_{L_2}}{\Gamma_{L_3}}\left(\frac{E_{L_3}}{E_{L_2}}\right)^2. \tag{7}$$

Values for matrix elements can be found in Ref. 8, which allows us to estimate the scattering amplitudes and the ratio R. At the L_3 edge, we obtain $F_0^{L_3}=0.70\ r_0$ with $\Gamma=9$ eV as estimated from the fluorescence. At the L_2 edge we have $F_0^{L_2}=0.25\ r_0$ with $\Gamma=14$ eV. This leads to a ratio $R=-1.4$. The order of magnitude for the dipole resonant amplitudes can be estimated from Eq. (4). To make an approximate calculation, the parameter δ is estimated by scaling the value for gadolinium[8] by the ratio of the spin in uranium to that in gadolinium. This approximation is valid for the rare earths where the $4f$ orbitals are localized. This is probably not true for uranium for which the $5f$ states are more delocalized. However, the calculation is qualitative and allows a comparison with experiments. We have $\delta=0.12(3/2)/(7/2)\approx0.05$ and taking $n_h=9$ and $n_{d\uparrow}-n_{d\downarrow}=0.2$, the estimated dipole resonant amplitude for $\Delta=0$ is $8\times10^{-2}\ r_0$ at the L_3 edge and $6\times10^{-2}\ r_0$ at the L_2 edge, in rough agreement with experiment.

Quadrupole transitions should also be taken into account. The formal expression for the quadrupolar scattering amplitude can be written and is found to contain 13 distinct terms. Hill and McMorrow[28] have expressed the dipole and quadrupole contributions in an orthogonal basis suited for experiments to highlight the dependence of the scattering amplitudes on each component of the magnetic moment. In our case, where we only consider incident σ polarization, we have for the dipole transition:

$$f_{j,E1}^{XRES}|_{\sigma\to\sigma}=0, \tag{8}$$

$$f_{j,E1}^{XRES}|_{\sigma\to\pi}=-iF^{(1)}\,\sin(\theta)z_3, \tag{9}$$

and for the quadrupole term:

$$f_{j,E2}^{XRES}|_{\sigma\to\sigma} = ic_2F_{E2}^{(1)}t_2z_2 + i(F_{E2}^{(3)} - F_{E2}^{(1)})s_2z_2^3 - iF_{E2}^{(3)}s_2z_2(z_1^2 + z_3^2), \tag{10}$$

$$f_{j,E2}^{XRES}|_{\sigma\to\pi} = ic_2F_{E2}^{(1)}(-sz_3 + cz_1) - i(F_{E2}^{(3)} - F_{E2}^{(1)})(-c^3z_1^3 + sc^2z_1^2z_3 + s^2cz_1z_3^2 - s_2sz_1z_2^2 - s_2cz_3z_2^2 - s^3z_3^3)$$
$$- iF_{E2}^{(3)}(cc_2z_1z_2^2 + (s_2c + s^3)z_1^2z_3 - c_2sz_2^2z_3 + (c^3 + s_2s)z_1z_3^2 + cs^2z_1^3 + c^2sz_3^3), \tag{11}$$

where z_i is the projection of the magnetization unit vector on the orthogonal basis of Hill and McMorrow with the shorthand notation $c=\cos(\theta)$, $c_2=\cos(2\theta)$, $c^2=\cos^2(\theta)$, etc. The $F_{E2}^{(1)}$ and $F_{E2}^{(3)}$ may be related to the values calculated by Hamrick[8] and are a few $10^{-2}\ r_0$ at both edges. The order of magnitude for quadrupole amplitude is therefore similar to that for dipole terms.

To distinguish between dipole and quadrupole transitions, we use the following considerations. For a specular $(0\ 0\ l)$ reflection or an off-specular one of the form $(h\ 0\ l)$, $z_2=0$ and the unrotated $\sigma\to\sigma$ channel is forbidden for both dipole and quadrupole transitions. To detect a resonant magnetic signal in the unrotated $\sigma\to\sigma$ channel in case of a quadrupole transition, we have to set the diffractometer in a geometrical configuration for which the ordered moment has a nonzero z_2 component. In our case, this can be achieved by measuring $(0\ k\ l)$ reflections for which

$$z_2 = \sin(\chi) = \frac{kc}{la}, \tag{12}$$

and $f_{j,E2}^{XRES}|_{\sigma\to\sigma}$ in Eq. (10) can be made finite. The relative intensity in the $\sigma\to\sigma$ and $\sigma\to\pi$ channels depends on the ratio $F_{E2}^{(3)}/F_{E2}^{(1)}$, in addition to the scattering angle.

Numerical simulations were made for different values of the $F_{E2}^{(3)}/F_{E2}^{(1)}$ ratio for several reflections in order to determine their angular dependence and relative intensities in both polarization channels. Figure 10 shows the square of the scattering amplitude for the (0 4 17) for the two polarization channels as a function of $F_{E2}^{(3)}/F_{E2}^{(1)}$. We note that the expected intensity for this reflection is similar in both channels for any ratio $F_{E2}^{(3)}/F_{E2}^{(1)}$ smaller than 1. The vertical line corresponds to the predicted value for $F_{E2}^{(3)}/F_{E2}^{(1)}$.[8] Considering

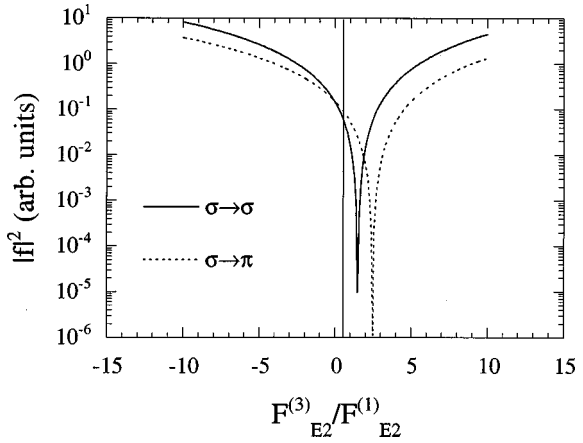

FIG. 10. Square of the scattering amplitude for the $(0\ \bar{4}\ 17)$ Bragg peak in both $\sigma\to\sigma$ and $\sigma\to\pi$ polarization channels as a function of the quadrupole atomic factors ratio $F_{E2}^{(3)}/F_{E2}^{(1)}$.

now only specular reflections with $z_1=z_2=0$, i.e., $z_3=1$, it is easy to see from Eq. (11) that the angular dependence of the scattering amplitude for the quadrupole transition in $\sigma\to\pi$ is a sine function for $F_{E2}^{(3)}/F_{E2}^{(1)}=-0.5$. In this particular case, the angular dependence of integrated reflections for both dipole and quadrupole transitions is identical and it is not possible to use this method to distinguish the two contributions. Simulations of intensities using Eqs. (10) and (11) with $F_{E2}^{(3)}/F_{E2}^{(1)}=-0.5$ give similar amplitudes in the $\sigma\to\sigma$ and $\sigma\to\pi$ channels for the off-specular reflections that we measured (0 1 12), (0 2 13), (0 2 15), (0 3 16), and (0 4 17).

B. Data analysis

At the L_3 edge, the temperature dependence of the $(0\ \bar{2}\ 15)$ in Fig. 5 does not indicate any change in intensity above background in the $\sigma\to\sigma$ channel, whereas a signal develops in the $\sigma\to\pi$ channel below the ordering temperature. This indicates its magnetic origin. The dipolar origin of the resonant scattering process is evidenced by the Q dependence of the specular reflections measured at different Bragg angle as shown in Figs. 6 and 9, where the solid line corresponds to the expected sine function for the scattering amplitude [see Eq. (9)].

As discussed above, quadrupolar terms can mimic the Q dependence of dipolar terms if the two parameters $F_{E2}^{(3)}$ and $F_{E2}^{(1)}$ are such that $F_{E2}^{(3)}/F_{E2}^{(1)}=-0.5$. However, with such a ratio, the magnetic intensity in both channels would be of the same order for the (0 2 15) off-specular reflection and some intensity should appear above the background in the $\sigma\to\sigma$ channel. As nothing is detected within our experimental sensitivity, we can conclude that the magnetic enhancement of the signal at the uranium L_3 edge is due to dipole transitions only. The similar results observed at the L_2 edge lead to the conclusion that the resonance is also dipole at this edge. This means that the scattering process at the uranium $L_{2,3}$ edges in UPd_2Si_2 is sensitive to the spin polarization of the $6d$ band.

Having demonstrated that the resonance has a dipolar origin at the $L_{2,3}$ edges, we can turn to the energy dependence. At the uranium L_3 edge, the solid line in the lower frame of Fig. 4 corresponds to a fit of the sum of two scattering amplitudes centered at different resonant energies $E_{L_3^1}$ and $E_{L_3^2}$. The linewidth Γ is obtained from the analysis of the absorption coefficient curve.[29,30] The fluorescence can be represented as a superposition of Lorentzian resonances and a contribution from the continuum. If we assume that the absorption edge and the white line have the same width, we determine a value for $\Gamma=8.5$ eV. The dashed line in the upper part of Fig. 4 corresponds to this description. The Γ value is higher than the one given in Ref. 31, but smaller than any of the ones tabulated for several uranium compounds by Kalkowski *et al.*[32] A value for f'' at the edge can

be obtained from the resonant contributions. At the L_3 edge, this leads to $4.5r_0$. This is to be compared with the estimation for dipolar transitions [Eq. (3)] together with values for the radial matrix elements[8] and $n_h \approx 9$, which gives roughly $6r_0$, in good agreement with our measured value. The predicted quadrupole contribution amounts to $\approx 0.5r_0$.[8]

The two magnetic contributions observed at the L_3 edge are separated by approximately 8 eV and the amplitude of the high-energy component is about 3.5 times weaker than the main resonance. A similar behavior has been observed in x-ray-absorption-edge spectra of mixed-valence rare-earth compounds where a second contribution appears about 8 eV above the main peak.[33] The two peaks may represent the two states available in a mixed-valence material and the shift in energy corresponds to the difference in Coulomb interaction between the $2p_{3/2}$ core hole and the $5f$ electronic states. Kalkowski *et al.* found a shift of only 4 eV in UO_3, incompatible with the 8 eV observed in rare-earth compounds and invoked a multiple-scattering resonance to explain the uranium absorption spectra. Another reason could be related to the density of states of the $6d$ bands at the Fermi level in the presence of the $2p_{3/2}$ core hole. It is known that the L_3 edge probes the total $6d$ band[34] and additional channels in this band could explain the second resonance.

At the L_2 edge, the core hole life time $\Gamma = 14$ eV has been estimated by analyzing the absorption coefficient measurement as discussed above. The value is larger than the one tabulated by Krause and Oliver[31] but in good agreement with that from Bambynek *et al.*[30] At the L_2 edge, f'' reaches $2.3r_0$, in excellent agreement with the value of $2.5r_0$ estimated from the resonant term in Eq. (5). Again, the predicted quadrupole contribution is much weaker, $0.16r_0$.[8] The energy line shape of the magnetic reflectivity of the (0 0 13) Bragg peak in Fig. 8 is described with two resonances, one for the spin-up and one for the spin-down $6d$ bands, separated by an energy Δ. The solid line corresponds to a splitting of $\Delta = 1$ eV. The ratio of the amplitude A_1 of the lower energy spin-up band to the amplitude A_2 of the higher energy spin-down band is -0.95, which gives a value

$$\frac{A_1 - A_2}{A_1 + A_2} = \frac{1 + 0.95}{1 - 0.95} \approx 40. \tag{13}$$

In this model, the polarization factor P in Eq. (4) can be written as

$$P = (A_1 + A_2) + \frac{(A_1 - A_2)\Delta/\Gamma}{(E_{L_3} - \hbar\omega)/(\Gamma/2) - i}, \tag{14}$$

in the limit of small Δ/Γ. The amplitude ratio in Eq. (14) can be compared with the ratio $-n_h/[(n_{d\uparrow} - n_{d\downarrow}) - n_h\delta]$ obtained from Eq. (4) With $\delta \approx 0.05$, $n_h = 9$ and $n_{d\uparrow} - n_{d\downarrow} = 0.2$, we get about 36, in good agreement with the measured value.

The different energy line shape of the L_3 and the L_2 edge could arise from the different transition probabilities from the core orbitals to the uranium $6d$ electronic states. Transitions at the L_3 edge probe the whole $6d$ band, while the L_2 edge is sensitive to $6d_{3/2}$ states only. The observed value of R^2 is ≈ 5, which differs from the estimated value of $(-1.4)^2 \approx 2$. It should be emphasized that an inverse intensity ratio has been observed at the $L_{2,3}$ edges in most elements of the light $4f$ series.[35] In neodymium, with three electrons in the $4f$ shells, $R^2 = 1/6$ for metallic Nd (Ref. 35) and $R^2 \sim 1/100$ for ionic Nd^{3+} in Nd_2CuO_4.[36] Calculations of the circular dichroic intensity at the $L_{2,3}$ edges also indicate larger L_2 enhancements for less than half-filled electronic $4f$ configurations.[9]

The position of the maximum of the magnetic intensity in the resonant profile at these two L edges is different from what has been observed at the M_4 edge in UPd_2Si_2 (Ref. 37) and other uranium systems[6,38] where the peak in the resonant profile appears approximately at the same energy as the peak in the absorption spectrum. The white-line peak in the absorption curves corresponds to the mean energy difference of the core level and unoccupied $6d$ states, while the magnetic contribution may have a significant correction due to Δ. This may induce a shift of few eV at the L edges.

V. CONCLUDING REMARKS

In these experiments we have studied the resonant x-ray scattering processes at the uranium L_2 and L_3 edges. The resonant energy profiles observed at the L_2 and L_3 edges are different. A single resonance is observed at the L_2 edge. The L_3-edge line shape can be represented by two terms, both of the dipolar type. The scattering amplitudes calculated from the measured integrated reflectivities are in qualitative agreement with the estimates for dipole transitions.

The polarization analysis of magnetic scattered intensities reveals no contribution in the unrotated polarization channel for any of the measured reflections. The temperature dependence of the scattered intensity of selected magnetic reflections confirms the absence of a magnetic signal in this channel. Furthermore, the magnetic integrated intensities of specular reflections at three different energies reveal the characteristic angular dependence expected for dipole transitions. We conclude that the scattering process at the uranium L_2 and L_3 edges is of the dipolar type. This provides a tool to study the $6d$ magnetism independently of the $5f$ moments that are probed at the uranium M_4 and M_5 edges.

ACKNOWLEDGMENTS

The help of L. Chabert and R. Chagnon during experiments is fully acknowledged.

*Present address: X-MAS, British CRG, ESRF, Grenoble.

†Permanent address: ISIS Facility, Rutherford Appleton Laboratory, Chilton, Didcot, Oxfordshire, OX11 0QX, United Kingdom.

[1] L. M. Sandratskii and J. Kübler, Phys. Rev. B **50**, 9258 (1994).

[2] J. Rossat-Mignot, G. H. Lander, and P. Burlet, in *Handbook on the Physics and Chemistry of the Actinides*, edited by A. J. Freeman and G. H. Lander (Elsevier, Amsterdam, 1984).

[3] D. Gibbs, Synchrotron Radiat. News **5**, 18 (1992).

[4] C. Vettier, in *Resonant Anomalous X-Ray Scattering Theory and Applications*, edited by G. Materlik, C. J. Sparks, and K. Fischer (Elsevier, Amsterdam, 1994).

[5] D. B. McWhan, J. Synchrotron Radiat. **1**, 83 (1994).

[6] D. B. McWhan, C. Vettier, E. D. Isaacs, G. E. Ice, D. P. Siddons, J. B. Hastings, C. Peters, and O. Vogt, Phys. Rev. B **42**, 6007 (1990).
[7] J. P. Hannon, G. T. Trammell, M. Blume, and D. Gibbs, Phys. Rev. Lett. **61**, 1245 (1988).
[8] M. D. Hamrick, Ph.D. thesis, Rice University, 1994.
[9] M. van Veenendaal, J. B. Goedkoop, and B. T. Thole, Phys. Rev. Lett. **78**, 1162 (1997).
[10] S. Langridge, J. A. Paixão, S. A. a. Sørensen, C. Vettier, G. H. Lander, D. Gibbs, A. Stunault, D. Wermeille, N. Bernhoeft, and E. Talik (unpublished).
[11] B. Shemirani, H. Lin, M. F. Collins, C. V. Stager, J. D. Garrett, and W. J. L. Buyers, Phys. Rev. B **47**, 8672 (1993).
[12] D. Wermeille, C. Vettier, N. Bernhoeft, A. Stunault, and P. Lejay (unpublished).
[13] M. S. S. Brooks (private communication).
[14] A. Vernière, S. Raymond, J. X. Boucherle, P. Lejay, B. Fåk, J. Flouquet, and J. M. Mignot, J. Magn. Magn. Mater. **153**, 55 (1996).
[15] A. Vernière, Ph.D. thesis, Université J. Fourier, Grenoble, 1995.
[16] A. Stunault, C. Vettier, F. de Bergevin, N. Bernhoeft, V. Fernandez, S. Langridge, E. Lidström, J. E. Lorenzo-Diaz, D. Wermeille, L. Chabert, and R. Chagnon, J. Synchrotron Radiat. **5**, 1010 (1998).
[17] F. Vaillant, Acta Crystallogr., Sect. A: Cryst. Phys., Diffr., Theor. Gen. Crystallogr. **52**, 967 (1977) [in French]. This paper contains the matrix representation for polarization analysis based on the use of analyzer crystals.
[18] Nick Bernhoeft (unpublished).
[19] B. E. Warren, *X-Ray Diffraction* (Addison-Wesley, Reading, MA, 1969), p. 46.
[20] B. Lebech, in *Magnetic Neutron Diffraction*, edited by A. Furrer (World Scientific, Singapore, 1995), p. 58.
[21] C. J. Sparks, in *Synchrotron Radiation Research*, edited by H. Winick and S. Doniach (Plenum, New York, 1980), p. 459.
[22] S. Eisebitt, T. Böske, J.-E. Rubensson, and W. Eberhart, Phys. Rev. B **47**, 14 103 (1993).
[23] K. Dumesnil, A. Stunault, P. Mangin, C. Vettier, D. Wermeille, N. Bernhoeft, S. Langridge, C. Dufour, and G. Marchal, Phys. Rev. B **58**, 3172 (1998).
[24] F. de Bergevin and M. Brunel, Acta Crystallogr., Sect. A: Cryst. Phys., Diffr., Theor. Gen. Crystallogr. **52**, 314 (1981).
[25] J. Luo, G. T. Trammel, and J. P. Hannon, Phys. Rev. Lett. **71**, 287 (1993).
[26] M. Blume and D. Gibbs, Phys. Rev. B **37**, 1779 (1988).
[27] A. J. Freeman, J. P. Desclaux, G. H. Lander, and J. Faber, Phys. Rev. B **13**, 1168 (1976).
[28] J. P. Hill and D. F. McMorrow, Acta Crystallogr., Sect. A: Found. Crystallogr. **52**, 236 (1996).
[29] F. de Bergevin, M. Brunel, R. M. Galera, C. Vettier, E. Elkaim, M. Bessière, and S. Lefèbvre, Phys. Rev. B **46**, 10 772 (1992).
[30] W. Bambynek, B. Crasemann, R. W. Fink, U. H. Freund, H. Mark, C. D. Swift, R. E. Price, and P. V. Rao, Rev. Mod. Phys. **44**, 716 (1972).
[31] M. O. Krause and J. H. Oliver, J. Phys. Chem. Ref. Data **8**, 329 (1979).
[32] G. Kalkowski, G. Kaindl, W. D. Brewer, and W. Krone, Phys. Rev. B **35**, 2667 (1987).
[33] J. M. Lawrence, M. L. den Boer, R. D. Parks, and J. L. Smith, Phys. Rev. B **29**, 568 (1984).
[34] H. Ebert, Rep. Prog. Phys. **59**, 1665 (1996).
[35] D. Watson, E. M. Forgan, W. J. Nuttall, W. G. Stirling, and D. Fort, Phys. Rev. B **53**, 726 (1996), and references therein.
[36] J. P. Hill, A. Vigliante, D. Gibbs, J. L. Peng, and R. L. Greene, Phys. Rev. B **52**, 6575 (1995).
[37] D. Wermeille, Ph.D thesis, Ecole Polytechnique, Lausane, 1998.
[38] C. C. Tang, W. G. Stirling, G. H. Lander, D. Gibbs, W. Herzog, P. Carra, B. T. Thole, K. Mattenberger, and O. Vogt, Phys. Rev. B **46**, 5287 (1992).